ADCONIP 2014 Hiroshima

# Comparative Study of Subspace Identification Methods on the Tennessee Eastman Process under Disturbance Effects

Andreas Bathelt[1] and Mohieddine Jelali[2]

***Abstract*— In this paper, subspace identification methods are compared regarding their capability to cope with process disturbances occurring in complex plants. The Tennessee Eastman process is considered to be a realistic simulation model of chemical processes. The MOESP, N4SID and ORT methods as well as some of their variants are applied to data gathered from the process while being subject to random disturbances. Such disturbances cause the identification methods to have unforeseen difficulties in identifying the correct parameter values.**

## I. INTRODUCTION

In face of the inevitable existence of non-white disturbances to which large and complex industrial chemical processes are subjected (*e.g.* the ambient temperature and its influence on supporting processes like the supply of cooling water), the question of whether and to what extent the results of subspace identification methods are affected under these conditions is raised. The aim of this paper is the comparison and analysis of the results, which subspace identification methods are able to give under these conditions. Therefore, a realistic process model with sufficent complexity is required. Furthermore, the model needs to have the ability to influence the process with realistic disturbances. A model having the desired complexity and the structure to incorporate realistic process disturbances is the process model of the Tennessee Eastman process published in [1]. In this first investigation, the emphasis is on the possible variation of the identification results rather than on the identification of the process itself.

Although an effort to identify the Tennessee Eastman process by means of subspace identification methods was made in [2], no disturbances were used except for the measurement noise. A comparison of the different subspace identification approaches based on a comparable model like that of the Tennessee Eastman process has not been published since. Moreover, the comparison of the ORT (orthogonal decomposition) method of [3], which showed good results under conditions when the disturbing stochastic process has a different dynamic than the system to be identified, to methods like the N4SID (numerical algorithms for subspace state-space system identification) method of [4] is seldom done in the context considered here. Such a comparison was recently published against the background of an electrodynamic system in [5].

[1]Andreas Bathelt is with the Laboratory of Control Engineering and Mechatronics, Cologne University of Applied Science, Betzdorfer Straße 2, 50679 Cologne, Germany andreas.bathelt@fh-koeln.de

[2]Mohieddine Jelali is with the Laboratory of Control Engineering and Mechatronics, Cologne University of Applied Science, Betzdorfer Straße 2, 50679 Cologne, Germany mohieddine.jelali@fh-koeln.de

The paper is structured as follows. Section II contains a brief review of the used subspace identification methods. In Section III, an overview of the Tennessee Eastman process is given. The description of the simulation model and the identification, *e.g.* choice of the test signal, follows in Section IV. Identification results are given and discussed in Section V. Finally, Section VI is devoted to some closing remarks.

## II. SUBSPACE IDENTIFICATION METHODS

In the following section, three different approaches to the problem of identifying a system in form of the state space representation

$$x(t+1) = Ax(t) + Bu(t) + Ke(t) \tag{1a}$$
$$y(t) = Cx(t) + Du(t) + e(t) \tag{1b}$$

are briefly discussed. Other forms and an overall overview of subspace identification are given in [6]. The considered methods are the MOESP (multiple input multiple output output-error state space), the N4SID and ORT methods. The first method was derived from a purely statistical point of view, whereas the third one was derived in the framework of the stochastic realization theory. The second method lies between the other two as it uses elements of the realization theory as well as approach of the statistical (data) approach. However, the actual implementations of these methods work with real data and thus use the statistical approach.

### A. Notations and Projections

Following [3], [7], the input $u$ and output $y$ are considered to be weakly stationary, second-order processes. Based on this assumption, the spaces

$$\mathcal{U} = \overline{\text{span}}\{\cdots, u(t-1), u(t), u(t+1), \cdots\}, \tag{2}$$
$$\mathcal{Y} = \overline{\text{span}}\{\cdots, y(t-1), y(t), y(t+1), \cdots\} \tag{3}$$

can be defined. The overbar denotes the closure with respect to the inner product defined by $E\{\eta\xi\}$ , where $\eta, \xi \in \mathcal{U}$ and $E\{\cdot\}$ is the mathematical expectation[1]. Furthermore, let the subspaces

$$\mathcal{U}_t^- = \overline{\text{span}}\{\cdots, u(t-2), u(t-1)\} \tag{4}$$
$$\mathcal{U}_t^+ = \overline{\text{span}}\{u(t), u(t+1), \cdots\} \tag{5}$$

be generated by the past as well as the present and future values of $u$. The spaces $\mathcal{Y}_t^+$ and $\mathcal{Y}_t^-$ are equally described

[1]It has to be kept in mind that these spaces are spanned by measurable functions of the type $f\colon \Omega \to \mathbb{R}^n$. Hence, the ambient space $\mathcal{P} = \mathcal{Y} \vee \mathcal{U}$ is a subspace of $\mathcal{L}^2(\Omega)$.

by $y$. The bond between the case of the stochastic realization theory and the data approach is explained in [3].

Let $a$ be a random variable and $\mathcal{B} = \overline{\text{span}}\{b\}$ the span of the random variable $b$, then the orthogonal projection $\hat{E}\{a|\mathcal{B}\}$ is given by the conditional expectation [7]

$$\hat{E}\{a|\mathcal{B}\} = E\{a|b\} = \mu_a + \Sigma_{ab}\Sigma_{bb}^{-1}(b - \mu_b) \; . \tag{6}$$

Since both $a$ and $b$ are elements of an ambient space $\mathcal{H}$, there is also an projection onto the orthogonal complement of $\mathcal{B}$, calculated as

$$\hat{E}\left\{a|\mathcal{B}^{\perp}\right\} = a - \hat{E}\{a|\mathcal{B}\} = a - \mu_a - \Sigma_{ab}\Sigma_{bb}^{-1}(b - \mu_b) \; . \tag{7}$$

Now, let $\mathcal{C} = \overline{\text{span}}\{c\}$ be the span of a third random variable $c$ fulfilling the condition $\mathcal{B} \cap \mathcal{C} = \{0\}$. The oblique projection $\hat{E}_{||\mathcal{C}}\{a|\mathcal{B}\}$ of $a$ onto $\mathcal{B}$ along $\mathcal{C}$ is given by the conditional covariance matrices as [7]

$$\begin{aligned} \hat{E}_{||\mathcal{C}}\{a|\mathcal{B}\} =& E\left\{\hat{E}\left\{a|\mathcal{C}^{\perp}\right\}\hat{E}\left\{\mathcal{B}|\mathcal{C}^{\perp}\right\}\right\} \\ & \times E\left\{\hat{E}\left\{\mathcal{B}|\mathcal{C}^{\perp}\right\}\hat{E}\left\{\mathcal{B}|\mathcal{C}^{\perp}\right\}\right\}^{-1} b \\ =& \Sigma_{ab|c}\Sigma_{bb|c}^{-1} b \; . \end{aligned} \tag{8}$$

### B. MOESP

The (ordinary) MOESP algorithm presented in [8] models only the part of (1) which is driven by the exogenous input $u$. Using the observed input–output data over some time span $T$, two block Hankel matrices $U$ and $Y$ are formed; see [8]. These two matrices are decomposed using the LQ decomposition:

$$\begin{bmatrix} U \\ Y \end{bmatrix} = \begin{bmatrix} L_{11} & 0 \\ L_{21} & L_{22} \end{bmatrix} \begin{bmatrix} Q_1^T \\ Q_2^T \end{bmatrix} \; . \tag{9}$$

Using the orthogonal projection of $Y$ onto the orthogonal complement of $U$ (the finite time spaces are basically the same as the spaces spanned by the Hankel matrices; see [3])

$$\hat{E}\{\mathcal{Y}_{[t\ t+T]}|\mathcal{U}_{[t\ t+T]}^{\perp}\} = L_{22}Q_2^T \tag{10}$$

and the singular value decomposition

$$L_{22} = \begin{bmatrix} U_1 & U_2 \end{bmatrix} \begin{bmatrix} \Sigma_1 & 0 \\ 0 & \Sigma_2 \end{bmatrix} \begin{bmatrix} V_1^T & V_2^T \end{bmatrix} \tag{11}$$

of $L_{22}$, the extended observability matrix is derived as

$$\mathcal{O} = U_1\Sigma_1^{1/2} \; . \tag{12}$$

From this matrix, the matrices $A$ and $B$ of (1) can be computed. The matrices $B$ and $D$ are calculated using $U_2$, $L_{11}$ and $L_{21}$. The statistical properties of the MOESP algorithm are discussed in [9]. Since MOESP is only asymptotically unbiased for white noise input signals, two other algorithms using an instrumental variable approach are proposed in [9], [10]. These algorithms use the additional data of the input and output respectively. The PI-MOESP algorithm of [9] uses the past of the input (in relation to $U$ and $Y$ of (9)), whereas the PO-MOESP algorithm proposed in [10] uses the past of the input and the output. The prefixes *PI* and *PO* stand for "past input" and "past output". As indicated by the name, the MOESP methods are state-space methods for the identification of models in the OE (output error) structure.

### C. N4SID

The idea of the N4SID method is to identify the system given by (1), so that the subsystem driven by the exogenous input $u$ (refered to as the "deterministic" part) as well as the system driven by the noise $e$ (refered to as the "stochastic" part) will share the matrices $A$ and $C$. As explained in [4], the first step is the calculation of the space spanned by the states. Assuming freedom of feedback and sufficient richness of the input (see [3], [7]), this space is calculated through the oblique projection ($\vee$ denoting the vector sum)

$$\mathcal{X}_t^{+/-} = \hat{E}_{||\mathcal{U}_t^+}\{\mathcal{Y}_t^+|\mathcal{Y}_t^- \vee \mathcal{U}_t^-\} \; . \tag{13}$$

Since the numerical implementation yields not only a basis vector of $\mathcal{X}_t^{+/-}$, but also the extended observability matrix, the states of the "deterministic" system can be computed by means of the extended observability matrix and the outputs

$$\begin{aligned} y_d(t) &= \hat{E}\{\mathcal{Y}_t^+|\mathcal{Y}_t^- \vee \mathcal{U}\} \; , \\ y_d(t+1) &= \hat{E}\{\mathcal{Y}_{t+1}^+|\mathcal{Y}_{t+1}^- \vee \mathcal{U}\} \; . \end{aligned} \tag{14}$$

These states are used to solve a least-square equation of the type

$$\min_{A,C,B,D} \left\| \begin{bmatrix} x^d(t+1) \\ y(t) \end{bmatrix} - \begin{bmatrix} A & B \\ C & D \end{bmatrix} \begin{bmatrix} x^d(t) \\ y(t) \end{bmatrix} \right\|_2 \tag{15}$$

for the system matrices. The residuals are used for the calculation of the "stochastic" system and thus for the computation of $K$. For a discussion of the basic principles of the N4SID approach and its two variants, refer to [4]. The first algorithm follows the explanation given here. The second algorithms skips the step of (14) and solely uses (13) to calculate the states. Furthermore, a robust version of the first algorithm is given in [4]. In [11], it is shown that this robust algorithm and the PO-MOESP method compute the same matrices $A$ and $C$. Enforced by the oblique projection (13), the "stochastic" system and the "deterministic" system will share the system matrix $A$ and the output matrix $C$ making the model of the N4SID approach analogous to the ARMAX (autoregressive-moving-average structure with exogenous input) structure.

### D. ORT

In terms of the fundamental idea of the ORT method, the system to be identified is considered to be a stochastic system driven by an exogenous input [3]. Following this rationale, the output $y$ is decomposed into a "deterministic" component driven by the exogenous input and a "stochastic" component driven by a white noise sequence. The "deterministic" component $y_d$ is separated from $y$ by means of an orthogonal projection of the output on the space spanned by the input. With the assumption of freedom of feedback, that is

$$y_d(t) = \hat{E}\{y(t)|\mathcal{U}\} = \hat{E}\{y(t)|\mathcal{U}_{t+1}^-\} \; . \tag{16}$$

The "stochastic" component $y_s$ is subsequently given by the projection onto the orthogonal complement of $\mathcal{U}$. Thus, $y_s$ is described by

$$\begin{aligned} y_s(t) &= y(t) - \hat{E}\{y(t)|\mathcal{U}_{t+1}^-\} = y(t) - \hat{E}\{y(t)|\mathcal{U}\} \\ &= \hat{E}\{y(t)|\mathcal{U}^{\perp}\} \; . \end{aligned} \tag{17}$$

The following identification, which is a MOESP-like algorithm in case of the deterministic component, results in a combination of the two subsystems in a block-diagonal order ($d$: "deterministic" subsystem, $s$: "stochastic" subsystem)

$$\begin{bmatrix} x_d(t+1) \\ x_s(t+1) \end{bmatrix} = \begin{bmatrix} A_d & 0 \\ 0 & A_s \end{bmatrix} \begin{bmatrix} x_d(t) \\ x_s(t) \end{bmatrix} + \begin{bmatrix} B_d \\ K_s \end{bmatrix} \begin{bmatrix} u(t) \\ e(t) \end{bmatrix}, \quad (18a)$$

$$y(t) = \begin{bmatrix} C_d & C_s \end{bmatrix} \begin{bmatrix} x_d(t) \\ x_s(t) \end{bmatrix} + \begin{bmatrix} D_d \\ I \end{bmatrix} \begin{bmatrix} u(t) \\ e(t) \end{bmatrix}. \quad (18b)$$

This structure can be seen as the state-space analogue of the Box–Jenkins structure. For a thorough explanation of the ORT method the reader should refer to [7]. The basic description and some additional insight regarding the relationship between the algorithms used to derive the model using observed data and the underlying setting of stochastic realization theory are given in [3].

## III. TENNESSEE EASTMAN PROCESS

The Tennessee Eastman process was first introduced at the AIChE 1990 Annual Meeting in Chicago, Illinois, USA and was later published in [1]. It draws its relevance for case studies from the fact that it was modelled based on a real process.

The substance system of the process consists of 8 components named A through H. The components A, C, D and E are the reactants. Components G and H are the desired products. Component F is a by-product, while component B is an inert. The reactions as given in [1] are

$$\begin{aligned} \text{A(g) + C(g) + D(g)} &\rightarrow \text{G(liq)} && \text{product 1,} \\ \text{A(g) + C(g) + E(g)} &\rightarrow \text{H(liq)} && \text{product 2,} \\ \text{A(g) + E(g)} &\rightarrow \text{F(liq)} && \text{by-product,} \\ \text{D(g)} &\rightarrow \text{2F(liq)} && \text{by-product.} \end{aligned}$$

The piping and instrumentation diagram (P&ID) for the process is shown in Fig. 1. The major unit operations are the reactor, the product condenser, the vapour-liquid separator, the recycle compressor and the product stripper. The gaseous reactants A, D and E are fed directly into the reactor. Reactant C and also an amount of A (stream 4) enter the process through the stripper. After reacting, a blend of vaporous products and the unreacted feed leaves the reactor. Subsequently, this blend runs through the condenser where the vaporous components liquidify. After being separated in the vapour-liquid separator, the noncondensed components are fed back through the compressor to the reactor feed. In the downstream stripping column, the remaining reactants are removed using the components of feed stream 4 as stripping agents.

In the P&ID, the four-digit numbers of the measuring points and valves are assigned with respect to the five units. The first two digits specify the unit; 11 is for the reactor, 12 for the condenser, 13 for the separator, 14 for the compressor, 15 for the stripper and 10 is for the overall equipment.

Although an inert, component B affects the process. It is crucial that the amount of this component circulating in the process is kept constant. Hence, it needs to be purged from the process together with the by-product through stream 9.

## IV. SIMULATION AND IDENTIFICATION

Details of the simulation and subsequent identification are presented. The model of the Tennessee Eastman process stems from [14]. The operating mode of the plant model during the identification experiments was the base case (Mode 1; see [1]). The general simulation and identification parameters are listed in Table I. The implementational aspects are described in the following subsections.

TABLE I
SIMULATION AND IDENTIFICATION SPECIFICATIONS

| | |
|---|---|
| Solver (Fixed-step) | ode3 (Bogacki-Shampine) |
| Duration | 96 h |
| Step size | 0.5 s |
| Decimation (relative to step size) | 60 |
| Sample time of input signal | 30 s |
| Time span used for identification | 24 h - 96 h |
| Number of data points | 8640 |
| Sample Time of data points | 30 s |
| Number of block rows used for constructing the Hankel matrices | 75, 200* |

* only for the identifications of the reactor, separator, stripper and the MISO systems (see below)

### A. Simulation design

Due to its inherent instability, first the process needed to be stabilized. However, in order to preserve as much of the process dynamic as possible, the number of controllers added to the plant was kept to a minimum and controllers were solely used to prevent the plant from violating its shutdown constraints. In [12] a stabilization strategy is proposed. In terms of the stabilization of the reactor pressure an improvement can be achieved using the three-stage cascade control proposed in [13]. The reactor pressure is linked with the reactor temperature, since both values are dependent on each other through the reaction within the reactor. The implemented control loops are shown in Fig. 1. As a result of the process stabilization, not all manipulated variables as mentioned in [1] are accessible. On the other hand, the set points of the controllers constitute additional manipulated variables of the stabilized process. The resulting manipulated variables, which are considered as the system inputs during the identification, and their steady-state values of Mode 1 are presented in Table II. The outputs of the models are the usual outputs as given in Table 4 and Table 5 of [1, p. 249].

Since an examination of the effects of process disturbances is desired, some changes to the model of [14] are necessary. The model has been augmented with two additional parameters. The first parameter facilitates the initialization of the model's random generator, thereby allowing for simulation with different disturbance characteristics. By means of the second parameter, the measurement noise of the measuring points can be switched off. The process disturbances, which were activated during the simulations, are shown in Table III.

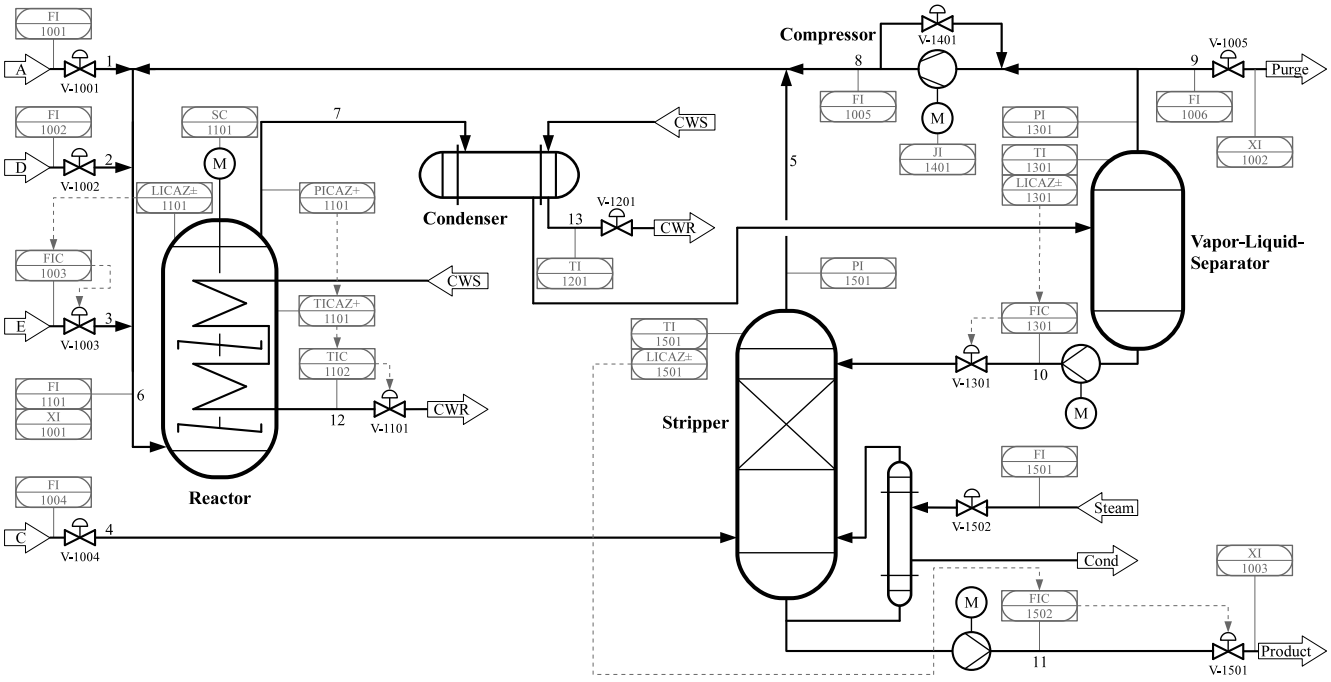


Fig. 1. Tennessee Eastman process (CWS: cooling water supply; CWR: cooling water return; Cond: condensate) with control loops for process stabilization (in accordance with explanations in [1], [12], [13])

TABLE II

MANIPULATED VARIABLES OF THE STABILIZED PROCESS AND VALUES OF THEIR RESPECTIVE INPUT SIGNALS

| P&ID identifier | Description | mean | variance |
|---|---|---|---|
| V-1002 | D feed (stream 2) | 63.053% | $6.25\%^2$ |
| V-1001 | A feed (stream 1) | 24.644% | $6.25\%^2$ |
| V-1004 | A and C feed (stream 4) | 61.302% | $6.25\%^2$ |
| V-1401 | Compressor recycle valve | 22.210% | $6.25\%^2$ |
| V-1005 | Purge valve (stream 9) | 40.064% | $6.25\%^2$ |
| V-1502 | Stripper steam valve | 47.446% | $6.25\%^2$ |
| V-1201 | Condenser cooling water flow (stream 13) | 18.114% | $6.25\%^2$ |
| SC 1101 | Agitator speed | 50% | $6.25\%^2$ |
| PICAZ+ 1101 | Setpoint reactor pressure (gauge pressure) | 2705 kPa | 625 $\text{kPa}^2$ |
| LICAZ± 1101 | Setpoint reactor level | 75% | $6.25\%^2$ |
| LICAZ± 1301 | Setpoint separator level | 50% | $6.25\%^2$ |
| LICAZ± 1501 | Setpoint stripper level | 50% | $6.25\%^2$ |

TABLE III

RANDOM VARIATION DISTURBANCES [1]

| Identifier in [1] | Description |
|---|---|
| IDV(8) | A, B, C feed composition of stream 4 |
| IDV(9) | D feed temperature of stream 2 |
| IDV(10) | C feed temperature of stream 4 |
| IDV(11) | Reactor cooling water inlet temperature |
| IDV(12) | Condenser cooling water inlet temperature |

### B. Identification

Throughout the simulations, the input signal was chosen to be a coloured noise sequence. It best meets the requirements of the identification problem at hand. Firstly, from the viewpoint of a realistic setting of the identification, it stresses the equipment less than other signal types like the pseudo-random binary signal. Rapid and step-like changes of the coloured noise can be avoided by using a suitable generation filter. Secondly, the number of block rows of the Hankel matrices can be changed at will without violating the requirements of sufficient (persistence of) excitation and the related rank conditions of these matrices. In terms of persistence of excitation, let a coloured noise sequence be described by an average representation

$$u(t) = \sum_{i=0}^{\infty} h(i)e(t-i)$$

with $e$ being a zero-mean, pairwise orthogonal, second-order process, *i.e.* a white noise process. Since the filter is assumed to be stable and of minimal phase, the following can be deduced. The spaces generated by $u$ and $e$ up to time $t$ are denoted by $\mathcal{U}_{t+1}^-$ and $\mathcal{E}_{t+1}^-$ respectively. Then, it follows from the Wold decomposition theorem that $\mathcal{U}_{t+1}^- = \mathcal{E}_{t+1}^-$. Now, let for some index $k < t$ the space $\mathcal{U}_{t+1}^-$ be decomposed into a subspace spanned by the past up to $k$ denoted as $\mathcal{U}_k^-$ and a subspace spanned by the future of $k$ (up to $t$) denoted as $\mathcal{U}_k^+$. Since $e$ is an orthogonal basis of $\mathcal{U}_{t+1}^-$, the conditions ($+$ denoting the direct sum)

$$\mathcal{U}_k^+ + \mathcal{U}_k^- = \mathcal{U}_{t+1}^- , \qquad \mathcal{U}_k^+ \cap \mathcal{U}_k^- = \{0\}$$

hold. Therefore, a coloured noise sequence fulfils the richness condition and is consequently persistently exciting of order infinity [3], [7].

The four following identification approaches were considered (MIMO: multiple input multiple output; MISO: multiple input single output):

1) 22-by-12-MIMO system with all outputs except for X1001, X1002, X1003 (model orders: 10, 15)
2) 11-by-12-MIMO system with T1101, L1101, P1101, T1301, L1301, P1301, T1501, L1501, P1501, F1502, F1006 (model order: 10)
3) 3-by-12-MIMO systems of the reactor, separator and stripper using temperature, level and pressure of each unit (model order: 5)
4) MISO systems of T1101, L1101, P1101, T1301, L1301, P1301, T1501, L1501, P1501 (model order: 5)

First, baseline simulations and identifications without any disturbances and measurement noise were conducted in order to get the "deterministic" behaviour of the model. The coloured noise was generated using the filter

$$C(z) = \sqrt{k}\frac{\sqrt{1-a^2}}{1-az^{-1}}, \quad T_{\text{sample}} = 30 \text{ s} \tag{19}$$

from [7, p. 262]. The parameter $a$ manipulates the covariance properties of the resulting coloured noise. Since the plant is rather slow in its dynamics and thus fast varying input signals would show no significant reaction in the outputs, $a$ was chosen to give a slowly varying signal. Its value was set to $0.95$, $0.99$, $0.995$ and $0.999$, resulting in four different covariance characteristics of the input noise. The parameter $k$ adjusts the variance of the driving white noise (assuming unit variance) and thereby sets up the amplitude of the inputs. The value of $k$ for each particular input is given in Table II. These values create input signals with an amplitude in the range of $\pm 5\%$ and $\pm 50$ kPa. For each of the four signal types, 10 simulation with different signal realizations were run.

Afterwards, the signal giving the best identification result was used for the simulations with disturbances and measurement noise. Simulations with 30 different disturbance and noise characteristics were done, *i.e.* 30 different initial values of the model's random generator were used. In order to evaluate the consequences of changes of the input amplitude, the input signals were set to 100%, 50%, 20% and 10% of their nominal amplitude. That is, one disturbance characteristic was used for the simulations with each of the four amplitudes of the input signal. The resulting models of the disturbed data are compared against the model of the disturbance-free signal.

The identification methods used were the (ordinary) MOESP method of [8], the PI-MOESP method of [9], the PO-MOESP of [10], the first algorithm and the robust algorithm of the N4SID method given in [4] as well as the ORT method described in [3], [7]. The actual implementation of the ORT, MOESP, and PO-MOESP methods used are these given in the appendix of [7]. For the implementation of the PI-MOESP method the PO-MOESP implementation was altered according to [9]. The algorithms of the two N4SID algorithms are those coming as an addition with [4].

## V. RESULTS AND DISCUSSION

The step responses of the baseline models of the first and second identification approach deviated from the step responses of the disturbance-free process model too strong to be used for the analysis of the effects of processes disturbances. Thus, the analysis is stated by means of the third and fourth identification approaches. Those facts were upheld by the scattering of the eigenvalues. For the former two identification approaches, no clear convergence was evident, whereas the eigenvalues of the latter two approaches converged to distinct positions. Regarding the quality of the step responses of the identified models, the N4SID algorithms gave the best fit.

In terms of the identifications with disturbances and noise, two possible results were expected. If the effects of the disturbances were insignificant compared to the input signals or possessed the same dynamic[2] as the process, the model would be an OE, ARMAX or Box-Jenkins model. However, if the disturbances had a significant effect on the process and possessed a different dynamic, a Box-Jenkins model would be identified. That is, either the identified models would be the same as the baseline model or at least the results of the ORT method would remained the same. Furthermore, with a decreasing amplitude of the input signal an increasing variation of the identification results was expected.

All results of the methods showed significant deviations from the baseline models throughout all models of the third and fourth identification approach. The deviations remained even when the number of block rows of the Hankel matrices was increased from 75 to 200. Those deviations manifest themselves in particular in the eigenvalues of the identified models. The overall picture of the shift of the eigenvalues remained the same irrespective of the amplitude of the input signal. In Fig. 2 and Fig. 3, the eigenvalues of the identified reactor models (third identification approach) are shown using the input signal with an amplitude of 100%. In conformance with [11], the eigenvalues of the PO-MOESP and the robust N4SID methods are the same. Hence they are shown in the same diagram. Except for the PI-MOESP method, whose results already showed a strong variation of the eigenvalues' position when the disturbance-free data was used, the shift of the position of the eigenvalues is evident. Furthermore, this shift shows a direction towards new eigenvalue positions in case of disturbances. The robust N4SID algorithm was at least able to yield models with an approximately good steady-state gain. The transient behaviour was nowhere near that of the undisturbed process, though.

Since neither an ARMAX method (N4SID), an OE method (MOESP) nor a Box-Jenkins method (ORT) was able to identify the process in presence of disturbance, the following hypothesis can be stated: due to the nature and the complexity of the process structure, the disturbances are capable of causing a significant change within the process's elementary

[2]More precisely: the dynamic of the identified noise model is the same as the dynamic of the identified process model.

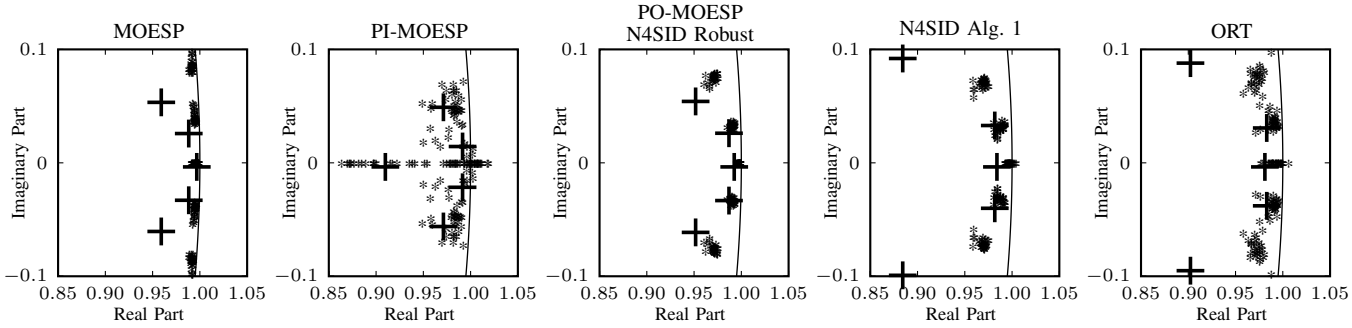


Fig. 2. Eigenvalues of the identification of the reactor using Hankel matrices with 75 block rows and $a = 0.995$ (cross: eigenvalues of the baseline model, asterisk: eigenvalues of the identification using the disturbed data)

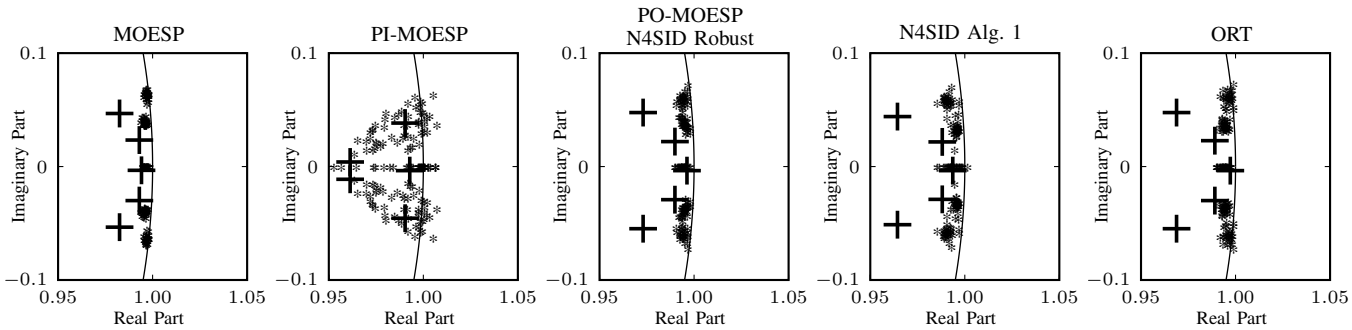


Fig. 3. Eigenvalues of the identification of the reactor using Hankel matrices with 200 block rows and $a = 0.995$ (cross: eigenvalues of the baseline model, asterisk: eigenvalues of the identification using the disturbed data)

dynamics (in terms of the identification methods), so that the presented methods are unable to determine the original (disturbance-free) behaviour of the process.

## VI. CONCLUSIONS

Using the Tennessee Eastman process as a representation of a complex process and a coloured noise signal as input to this process, it was shown that the subspace methods MOESP, N4SID and ORT cannot retrieve the underlying behaviour of the process when process disturbances are present. In order to verify or refute this hypothesis, two steps need to be taken. Firstly, the whole process needs to be analyzed in greater depth. Secondly, the number and type of identification experiments needs to be increased by considering additional input signals so as to remove possible effects due to correlation between the disturbances and input signals. As well, longer simulation times and additional disturbance characteristics will be considered. Finally, more identification methods will be used.

## REFERENCES


[1] J. J. Downs and E. F. Vogel, "A plant-wide industrial process control problem," *Computers & Chemical Engineering*, vol. 17, no. 3, pp. 245–255, 1993.

[2] B. C. Juricek, D. E. Seborg, and W. E. Larimore, "Identification of the Tennessee Eastman Challenge process with subspace methods," *Control Engineering Practice*, vol. 9, no. 12, pp. 1337–1351, 2001.

[3] G. Picci and T. Katayama, "Stochastic realiziation with exogenous inputs and 'subspace-methods' identification," *Signal Processing*, vol. 52, no. 2, pp. 145–160, 1996.

[4] P. van Overschee and B. De Moor, *Subspace Identification for Linear Systems: Theory, Implementation, Applications*. Boston and London and Dordrecht: Kluwer Academic Publishers, 1996.

[5] J. Zhang, C. Lu, and Y. Han, "MIMO identification of power system with low level probing tests: Applicability comparison of subspace methods," *IEEE Transactions on Power Systems*, vol. 28, no. 3, pp. 2907–2917, 2013.

[6] S. J. Qin, "An overview of subspace identification," *Computers & Chemical Engineering*, vol. 30, no. 10-12, pp. 1502–1513, 2006.

[7] T. Katayama, *Subspace methods for system identification*. London: Springer, 2005.

[8] M. Verhaegen and P. Dewilde, "Subspace model identification: Part 1. the output-error state-space model identification class of algorithms," *International Journal of Control*, vol. 56, no. 5, pp. 1187–1210, 1992.

[9] M. Verhaegen, "Subspace model identification: Part 3. analysis of the ordinary output-error state-space model identification algorithm," *International Journal of Control*, vol. 58, no. 3, pp. 555–586, 1993.

[10] M. Verhaegen, "Identification of the deterministic part of MIMO state space models given in innovations form from input-output data," *Automatica*, vol. 30, no. 1, pp. 61–74, 1994.

[11] A. Chiuso and G. Picci, "On the ill-conditioning of subspace identification with inputs," *Automatica*, vol. 40, no. 4, pp. 575–589, 2004.

[12] T. J. McAvoy and N. Ye, "Base control for the Tennessee Eastman problem," *Computers & Chemical Engineering*, vol. 18, no. 5, pp. 383–413, 1994.

[13] T. J. McAvoy, N. Ye, and C. Gang, "An improved base control for the Tennessee Eastman problem," in *Proceedings of the 1995 American Control Conference*, IEEE, vol. 1. Piscataway: IEEE, 1995, pp. 240–244.

[14] N. L. Ricker, "Tennessee Eastman Challenge archive," 2005. [Online]. Available: http://depts.washington.edu/control/LARRY/TE/download.html